

Co-pyrolysis of biosolids with alum sludge: Effect of temperature and mixing ratio on product properties

Nimesha Rathnayake^a, Savankumar Patel^{a,b}, Pobitra Halder^{a,b}, Shefali Aktar^a, Jorge Pazferreiro^a, Abhishek Sharma^c, Aravind Surapaneni^{b,d}, Kalpit Shah^{a,b,*}

^a Chemical & Environmental Engineering, School of Engineering, RMIT University, Melbourne, Victoria 3000, Australia

^b ARC Training Centre on Advance Transformation of Australia's Biosolids Resources, RMIT University, Bundoora 3083, Australia

^c Department of Chemical Engineering, Manipal University Jaipur, Jaipur, Rajasthan 303007, India

^d South East Water, Frankston, Victoria 3199, Australia

ARTICLE INFO

Keywords:

Biosolids
Alum sludge
Pyrolysis
Co-pyrolysis
Biochar
Heavy metals

ABSTRACT

Sustainable management of biosolids and alum sludge are becoming increasingly important due to the rapid growth in their production with increasing urbanization globally. Pyrolysis has been identified as a promising method for biosolids management. However, land application of biochar derived from pyrolysis of biosolids may be limited despite their significant agro-environmental benefits, mainly due to the potential increased concentration of heavy metal content in the biochar. Current study experimentally investigated co-pyrolysis of biosolids with alum sludge with an aim to produce high quality biochar with reduced heavy metal content. Moreover, it is further hypothesized that the addition of alum sludge may catalyze pyrolysis reactions, which may alter properties of pyrolysis products such as oil, gas and biochar. The results indicate that co-pyrolysis can reduce heavy metal concentrations in biochar while also improving oil and gas product qualities, suggesting beneficial synergistic effects. Furthermore, the process parameters such as pyrolysis temperature and alum sludge mixing ratio have a significant impact on the yield distribution and product (biochar, pyrolysis oil and gas) properties.

1. Introduction

Global biosolids generation rapidly rises due to exponential increase in urbanization and industrialization [1]. Biosolids are the treated solid organic by-product of wastewater, and conventional disposal methods of biosolids such as landfilling, stockpiling, and incineration are not environmentally sustainable. Increasing biosolids production and strict environmental regulations are causing the wastewater industries to move towards more sustainable management options [2]. Biosolids have great potential as a fertilizer in agricultural applications as it consists of organic compounds, macronutrients. Biosolids also consists of a wide range of the undesirable properties in biosolids such as odor, pathogens, heavy metals, pesticides, pharmaceutical waste, and other emerging contaminants such as micro-plastics and per fluoro alkyl substances (PFASs) [2–5].

Pyrolysis is considered as a promising method for sustainable management of biosolids [4–6]. It transforms biosolids at high temperatures (400–1200 °C) in the absence of oxygen to produce biochar, oil and gas products which may have potential applications as fuels [6,7]. Pyrolysis

eliminates odor, pathogens, micro-plastics, pesticides and pharmaceutical related impurities in the resultant biochar products [4–6]. It is also reported in the literature that PFASs may be vaporized at pyrolysis temperatures [8]. Hence biochar produced from biosolids may be free of PFAS. Furthermore, biochar has many benefits, especially in land applications as it improves soil carbon storage, improves the nutrient supply for plants, enhances the soil water retention capacity due to its porous nature and adsorbs soil pollutants. Biochar land application can also contribute to attenuate climate change by reducing N₂O, CH₄, and CO₂ emissions [9].

However, pyrolysis does not generally reduce heavy metals in biochar. On the contrary, biochar pyrolysis typically increases the concentration of the heavy metals, as most of the heavy metal present in biosolids retains in biochar while organic matter decomposes at pyrolysis temperatures [1,4,9]. High heavy metal content in biochar may limit its land applications as it could lead to soil contamination and associated risks to humans and the ecosystem [4,10]. There are strict rules and regulations globally around the land application of biosolids and their potential derivatives, which may reduce the market value of

* Corresponding author at: Chemical & Environmental Engineering, School of Engineering, RMIT University, Melbourne, Victoria 3000, Australia.
E-mail address: kalpit.shah@rmit.edu.au (K. Shah).

<https://doi.org/10.1016/j.jaap.2022.105488>

Received 22 October 2021; Received in revised form 26 January 2022; Accepted 1 March 2022

Available online 7 March 2022

0165-2370/© 2022 Elsevier B.V. All rights reserved.

biochar produced from biosolids [2,11].

Co-pyrolysis, therefore can be considered a promising technique to improve biosolids derived biochar quality by reducing heavy metal concentrations. Co-pyrolysis demonstrates great potential as a developing technique due to its simplicity and effectiveness. In co-pyrolysis, the mixture of two or more materials are used as the feedstock to perform pyrolysis, and it can be used to produce high-quality biochar by blending biosolids with other biomass that have low metal concentrations which dilutes the metal concentrations in the resultant biochar [1, 9,12–14]. There are numerous studies on co-pyrolysis of various lignocellulosic biomass as a method to improve the characteristics of pyrolysis oil, and to reduced production cost but literature on co-pyrolysis of biosolids is scarce [12,15–19]. Only few studies investigated co-pyrolysis of biosolids to improve biochar quality and those studies used lignocellulosic biomass such as cotton stalk, bamboo sawdust, and rice straw to blend with biosolids [1,9,13,20]. Therefore, it is important to investigate the potential of utilizing other types of waste as feedstock in co-pyrolysis with biosolids.

In this study, alum sludge, which is a by-product from water purification process, is identified as a potential feedstock for co-pyrolysis of biosolids. Drinking water treatment plants commonly use aluminum based coagulant agents such as aluminum sulfate (alum) and poly aluminum chloride. The sludge resulted from this process is removed after flocculation tanks which is commonly referred to as alum sludge [21]. Increasing volumes of alum sludge are generated around the world due to the increasing global demand for drinking water [22]. Most of the generated alum sludge is stockpiled or disposed into sewers and landfills. Hence, there is an identified requirement to investigate the potential beneficial applications to manage alum sludge [22]. Alum sludge also contains a low concentration of heavy metals and a substantial amount of minerals [22]. Co-pyrolysis of biosolids with alum sludge may produce high-quality biochar with lower heavy metal content, which has not been discussed in literature earlier.

In this study, suitability of co-pyrolysis of biosolids with alum sludge to produce biochar was investigated at different co-pyrolysis temperatures and mixing ratios. Biochar, oil and gas products from pyrolysis and

co-pyrolysis products from biosolids and alum sludge were characterized and the effect of the pyrolysis/co-pyrolysis temperature and mixing ratio of alum sludge on product properties and synergistic effects observed in co-pyrolysis of biosolids with alum sludge were also discussed.

2. Material and methods

Biosolids samples used in this study are supplied from Mount Martha Water Recycling Plant (38°16'06"S and 145°03'31"E) of South East Water Corporation, Victoria, Australia. In this plant, municipal and industrial sewage are treated using activated sludge process and anaerobic digestion followed by dewatering and solar drying before being stockpiled. The alum sludge sample employed in this study was sourced from the White Swan Water Treatment Plant (37°30'58"S 143°55'34"E) of Central Highlands Water, Victoria, Australia. In this plant aluminum sulfate (alum) is used as the coagulant and lime is used to optimize coagulation pH.

Biosolids and alum sludge materials were grinded using ball mill and sieved using a sieve shaker to obtain particles in the size range between 100 μm and 300 μm . Particle size distributions (Supplementary data-Fig. S1) of sieved biosolids and alum sludge samples were obtained using Malvern Mastersizer 3000 and samples were dried overnight at 150 °C in the oven (Binder FED 720 drying oven with air ventilation via a rear exhaust; Binder GmbH, Germany) prior to experiments.

Co-pyrolysis and pyrolysis experiments were carried out in a fluidized bed reactor constructed of a quartz tube. The reactor inner diameter was 27 mm and its reaction zone height was 680 mm. The distributor plate was located 320 mm above the bottom of the reactor and had a porosity of 3 (16–40 μm). Fig. 1 shows the experimental set up, which was used to carry out fluidized bed experiments pyrolysis and co-pyrolysis experiments. The reactor was operated at atmospheric pressure and the reactor was heated using an electric heating furnace at a 35 °C/min heating rate. The system was continuously fed with a stream of nitrogen to maintain the reactor in a minimum fluidization regime. After the set pyrolysis temperature was reached, each pyrolysis/co-

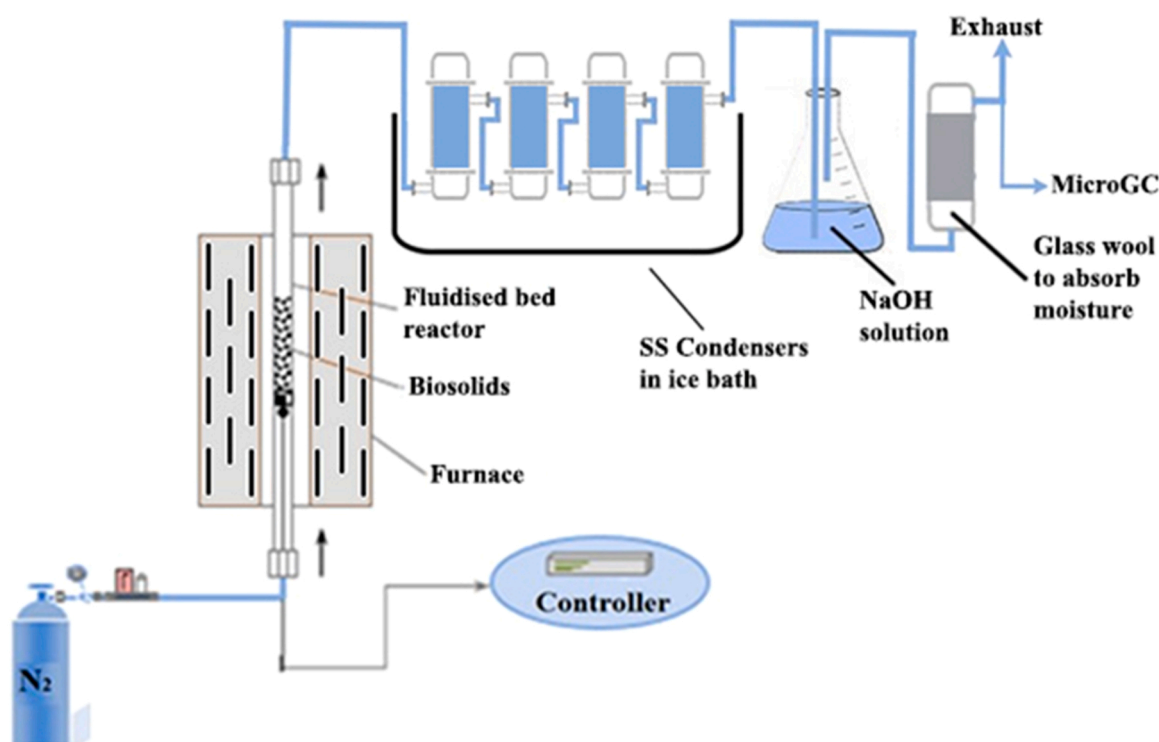


Fig. 1. Experimental setup for fluidized bed pyrolysis/co-pyrolysis.

pyrolysis experiment was carried out for 1 h, and after each experiment, biochar was collected from the reactor and pyrolysis oil was collected from the condensers. Pyrolysis gas was analyzed by a micro-GC equipment connected online.

Pyrolysis experiments of biosolids and alum sludge were carried out at three pyrolysis temperatures (500 °C, 700 °C and 900 °C). Co-pyrolysis experiments were carried out at two mixing ratios, which are biosolids: alum sludge 1:1 and biosolids: alum sludge 3:1 at temperatures 500 °C, 700 °C and 900 °C. In total, 12 experiments were carried out. Biosolids pyrolysis alone at X (X denotes temperature in °C) were labeled BSX, and alum sludge pyrolysis X (°C) were labeled ASX. Co-pyrolysis experiments of alum sludge and biosolids with a 1:1 mixing ratio at X (°C) were labeled AS: BS 1:1X, and co-pyrolysis experiments of alum sludge and biosolids with 3:1 mixing ratio at X (°C) were labeled AS: BS 3:1X.

Mass of biochar was calculated by subtracting the reactor's initial weight from the final weight after pyrolysis/co-pyrolysis. Biochar mass yield was calculated by Eq. 1;

$$\text{Biochar mass yield (\%)} = \frac{\text{Mass of biochar produced from pyrolysis/Co-pyrolysis}}{\text{Mass of feedstock used in pyrolysis}} \times 1 \quad (1)$$

Pyrolysis oil mass was calculated by subtracting the initial weights of condensers, pipes and heating coil from the final weight after pyrolysis/co-pyrolysis. Pyrolysis oil mass yield was calculated by Eq. 2.

$$\text{Pyrolysis oil mass yield (\%)} = \frac{\text{Mass of pyro oil produced from pyrolysis/Co-pyrolysis}}{\text{Mass of feedstock used in pyrolysis}} \times 100 \quad (2)$$

Pyrolysis gas mass yield was calculated as below shown in Eq. 3;

$$\text{Pyrolysis gas mass yield (\%)} = 100 - \text{Biochar mass yield} - \text{Pyrolysis oil mass yield} \quad (3)$$

Heavy metals (As, Cd, Cr, Cu, Ni, Pb, Se and Zn) in biosolids, alum sludge and biochar produced from pyrolysis and co-pyrolysis were determined by following U.S. EPA 3050B method [25]. Samples were digested using a water bath, and heavy metal concentration was determined using an inductively coupled plasma optical emission spectrometry (ICP-OES; Optima 5300DV; Perkin Elmer, USA). Bioavailable fractions of selected heavy metals (Cd, Cu, Ni, Pb and Zn) in biosolids, alum sludge and resultant biochar were determined by DTPA extraction method as described in Lindsay and Norvell (1978), followed by ICPMS analysis [26]. Elemental compositions (C, H, N and S) in the feedstock

and biochar products were determined using an elemental analyser (PerkinElmer 2400 Series II CHNS/O). Volatile matter, Fixed Carbon content and Ash content of feedstock and biochar were determined using TGA Q500 IR thermo gravimetric analyser, and calorific values were determined using Bomb Calorimeter, 6400 Parr. pH values of biochar and raw materials were obtained by mixing biochar and deionized water (10:1 water: biochar ratio) and the mixtures were equilibrated for 1 h, and pH value was then measured using a pH meter [25]. Fourier Transform Infrared (FTIR) spectra of the biosolids, alum sludge and biochar derived from pyrolysis and co-pyrolysis were obtained using a Perkin Elmer Spectrum 100 FTIR instrument. FTIR spectra were obtained for the wavenumber range of 4000 – 600 cm⁻¹ with 32 scans and 4 cm⁻¹ resolution and absorbance selected as the y axis. Brunauer–Emmett–Teller (BET) surface area of the biochar samples were determined using gas sorption (BET) surface area, and porosity analyser (TriStar II 3020) and surface characteristics of biochar were further analysed using SEM (FEI Quanta 200 SEM) imaging.

Pyrolysis oil samples were collected from the condenser using

dichloromethane, and these samples were analysed using GC/MS (Agilent, GC-7890A, and MS-5975C) to determine the composition of bio oil samples. HP-5 capillary column (30 m length, 0.25 mm I.D. and 0.25 µm film thickness) was used in the GC/MS equipment, and the temperature program of the column was as followed: 45 °C for 4 min, increase to

250 °C at 10 °C/min and maintain the temperature for 5 min at 250 °C [5]. Helium gas was used as the carrier gas and the temperature of the ion source was set to 250 °C [5]. The relative composition of each

compound was determined by peak area normalization [8]. pH measurements of pyrolysis oil were made using a calibrated pH meter at room temperature. The electrode was immersed into the sample solution until a steady reading is reached. Outlet gas stream from the pyrolysis reactor system was analysed using an Agilent Micro GC 490 which was connected to the pyrolysis reactor system. Micro GC extracted gas samples from the outlet gas stream every 4 min for analysis.

Percentage retention of Na and K in biochar produced from pyrolysis and co-pyrolysis were calculated using Eq. 4. The concentrations of Na and K in biosolids and alum sludge were found using acid digestion followed by ICP-MS analysis as described in heavy metal analysis.

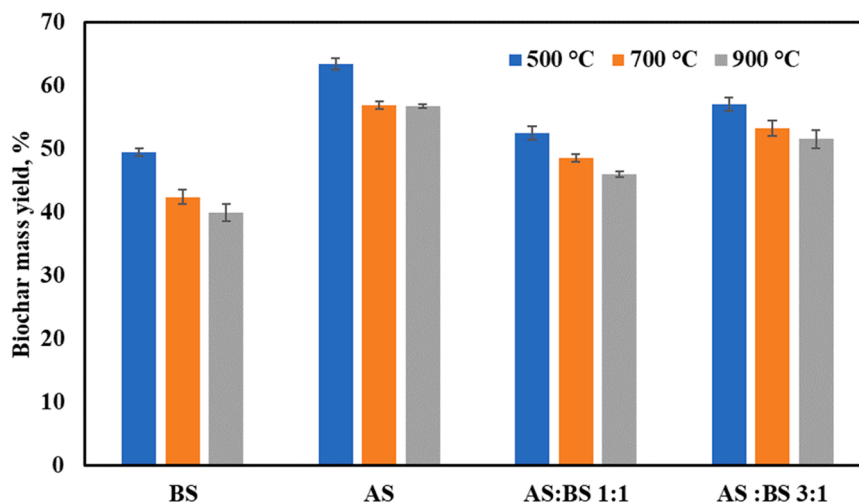


Fig. 2. Mass yield of biochar from pyrolysis/co-pyrolysis of alum sludge and biosolids at different pyrolysis temperatures (500 °C, 700 °C, and 900 °C).

$$\text{Alkali metal retention (\%)} = \frac{\text{Alkali metal concentration present in biochar} \times \text{Biochar yield}}{\text{Alkali metal concentration in the feed}} \times 100 \quad (4)$$

The higher heating value (HHV) of the pyrolysis gas is calculated by Eq. 5 below, where φ_i is the average molar percentages of CO, H₂, CH₄, C₂H₆, C₃H₈ [27].

$$\text{HHV (MJ/Nm}^3\text{)} = \frac{(\varphi_{\text{CO}} \times 12.633) + (\varphi_{\text{H}_2} \times 12.745) + (\varphi_{\text{CH}_4} \times 39.819) + (\varphi_{\text{C}_2\text{H}_6} \times 63.414) + (\varphi_{\text{C}_3\text{H}_8} \times 101.242)}{100} \quad (5)$$

The average relative deviation between the experimental value and calculated value was used to analyze synergetic effects in co-pyrolysis of biosolids and alum sludge on biochar, oil and gas product yields. Calculated product yield values for co-pyrolysis are calculated according to the following Eqs. 6 and 7,

For AS: BS 1:1 co-pyrolysis,

$$Y_{\text{calculated,(1:1)}, T,i} = \frac{Y_{\text{BS},T,i} + Y_{\text{AS},T,i}}{2} \quad (6)$$

For AS: BS 3:1 co-pyrolysis,

$$Y_{\text{calculated,(3:1)}, T,i} = \frac{Y_{\text{BS},T,i} + 3 \times Y_{\text{AS},T,i}}{4} \quad (7)$$

Where, $Y_{\text{calculated,(1:1)},T,i}$ is the calculated mass yield of *i* pyrolysis product (biochar, pyrolysis oil, and pyrolysis gas), of AS:BS 1:1 co-pyrolysis, at *T* temperature (500, 700 and 900 °C) and $Y_{\text{calculated,(3:1)},T,i}$ is the calculated mass yield of *i* product, of AS:BS 3:1 co-pyrolysis at *T* temperature. $Y_{\text{BS},T,i}$ is the experimental mass yield of *i* in biosolids at *T* temperature and $Y_{\text{AS},T,i}$ is the experimental mass yield of *i* in alum sludge.

The statistical analysis was performed using SPSS 15.0 on pyrolysis and co-pyrolysis yield accounting the effects of pyrolysis temperature and the effects of mixing ratio [5]. Turkey's test was used to differentiate

means within treatments ($P < 0.05$) [5]. The results of the statistical analyses can be found in Supplementary data (Table S2).

3. Results and discussions

3.1. Biochar yield and characterization

3.1.1. Biochar Yield

In Fig. 2, the yield of biochar produced from different feedstocks at different pyrolysis/co-pyrolysis temperatures are presented. It is observed that biochar yield decreased with increasing pyrolysis/co-pyrolysis temperatures in all pyrolysis and co-pyrolysis systems. For example, the yield of biochar derived from the pyrolysis of BS, AS, AS:BS (1:1) and AS:BS (3:1) at temperatures from 500° to 900°C were reduced by 21.94%, 12.04%, 12.30% and 8.04%, respectively. This trend is consistent with literature and can be attributed to the further decomposition of substances such as carbohydrates, protein, lipids, and polyphenols due to increased level of heat transfer at higher temperatures [5, 23,24].

Biochar yield from pyrolysis also varies with the original feedstock mixture. Biochar yield obtained from alum sludge, and alum sludge and biosolids mixtures were significantly higher compared to biosolids. Biochar yield also increased with increasing mixing ratio of alum sludge in the feedstock mixture. This can be mainly due to the higher ash content and less volatile matter content present in alum sludge when compared to biosolids. Most of the studies in literature reported a decrease in biochar yield in co-pyrolysis compared to pyrolysis of biosolids, but those studies have used feedstock with less ash content and high volatile matter, such as lignocellulose biomass and food waste as co-pyrolysis feedstock [9,23,24]. Therefore, alum sludge can be

Table 1
Heavy metal content in feedstocks and resultant biochar from pyrolysis and co-pyrolysis experiments and contaminant upper limits for classifying biosolids grade C1 and C2 according to EPA Victoria Biosolids Guidelines [25].

Metal Component Temperature	Metal content (mg/kg)														C1 Grade (mg/kg)	C2 Grade (mg/kg)
			500 °C				700 °C				900 °C					
	Biosolids	Alum sludge	BSBC	ASBC	AS:BS (1:1) BC	AS:BS (3:1) BC	BSBC	ASBC	AS:BS (1:1)BC	AS:BS (3:1) BC	BSBC	ASBC	AS:BS (1:1)BC	AS:BS (3:1) BC		
As	4.63	9.91	5.87	13.13	10.99	12.84	3.84	12.52	8.29	3.09	3.64	3.73	1.46	8.81	20	60
	±	±	±	±	±	±	±	±	±	±	±	±	±	±		
Cd	0.185	0.05	1.06	1.43	0.51	1.08	1.17	1.72	3.76	1.42	2.18	0.95	0.27	0.60	1	10
	1.10	< 0.1	1.72	0.30	1.10	0.50	1.50	0.21	0.80	0.50	1.30	0.28	0.9	0.4		
Cr	0.46		0.14	0.08	0.68	0.05	0.09	0.03	0.01	0.03	0.05	0.03	0.01	0.01	400	3000
	21.03	4.03	50.49 ±	8.41	23.69	16.93	55.56	11.65	26.7	15.91	60.00	12.60	28.32	19.33		
Cu	2.48	1.49	1.30	1.85	1.04	2.22	2.65	0.35	3.05	2.51	3.34	0.84	0.66	100	2000	
	1014.41	79.35 ±	1894.54	111.00	1181.65 ±	460.1	1998.47	119.78	968.14 ±	412.99 ±	1850	136.42	961.76 ±			494.24 ±
Ni	2.21	2.83	±	±	29.17	±	±	±	5.93	13.51	±	±	4.12	12.88	60	270
	8.83	12.12 ±	27.53	19.50	37.18	19.95	149.24	19.89	25	2.21	33.99	16.68	35.50	25.50		
Pb	1.59	0.97	3.89	1.41	1.71	3.99	1.91	5.76	1.53	0.51	0.66	2.25	0.25	300	500	
	23.03	±	50.13 ±	1.03	25.75	12.52	51.52	2.04	23.12	13.77	53.48	3.90	21.76			17.02
Se	±	2.06	3.66	±	±	±	±	±	±	±	±	±	±	3	50	
	2.02	0.935	0.87	2.14	3.28	1.53	0.98	5.11	2.65	0.98	2.08	1.45	1.87			
Zn	4.52	< 1	5.22	< 1	< 1	< 1	5.51	< 1	< 1	< 1	5.89	< 1	< 1	< 1	200	2500
	±	±	±	±	±	±	±	±	±	±	±	±	±			
Zn	0.30		0.3				1.2				0.9			200	2500	
	895.44	60.77 ±	1823.55	112.54	922.95 ±	413.50 ±	2230.16	145.31	955.31 ±	453.31 ±	518.16	93.76	767.88 ±			419.71 ±
	±	9.62	±	±	13.53	18.25	±	±	22.35	3.35	±	±	54.21	10.15		
	32.28		88.23	43.09			134.92	35.43			5.92	32.45				

BSBC = Biosolids biochar, ASBC = Alum sludge biochar, AS: BS (1:1) BC= Biochar from co-pyrolysis of alum sludge and biosolids at 1:1 mixing ratio, AS: BS (3:1) BC= Biochar from co-pyrolysis of alum sludge and biosolids at 3:1 mixing ratio

identified as a good feedstock to be blended with another feedstock to increase the biochar product yield. Moreover, the highest biochar yield from co-pyrolysis of alum sludge and biosolids was obtained when alum sludge and biosolids are co-pyrolyzed in a 3:1 ratio at 500 °C.

3.1.2. Total heavy metal concentration in biochar

The total concentration of heavy metals present in biosolids, alum sludge and biochar derived from pyrolysis of biosolids and alum sludge and their mixtures are presented in Table 1. Allowable limits of heavy metal concentrations in biosolids to be fit for land applications according to the EPA Victoria Biosolids Guidelines are also included in Table 1. EPA Victoria regulates the production, quality and use of biosolids to maximize their reuse while protecting the environment and public health [25]. Their guidelines classify biosolids into two main contamination grades based on the heavy metal concentration in biosolids [25]. C1 is the grade given to the least contaminated biosolids, and they are allowed to be used in unrestricted land applications [25]. It can be seen that heavy metals concentrations in biosolids feedstock varied in the sequence of Cu > Zn > Pb > Cr > Ni > As > Se > Cd. Concentrations of Cu, Zn, Cd and Se present in biosolids exceeded the allowable limits to be classified as C1, and thus land applications of biosolids are limited [25].

Biochar samples produced from pyrolysis had higher heavy metal concentrations compared to their original feedstock, and most of the heavy metals present in biochar displayed an enrichment trend with rising pyrolysis temperature. The total concentration of Cr, Ni, Cu, Zn, Se and Pb increased with increasing pyrolysis temperature up to 700 °C. These observations are consistent with literature and can be explained by the higher thermal stability of metals compared to organic compounds resulting nearly all the metals present in feedstock being retained in the biochar [1,13]. However, the behavior of Cd with rising temperature was distinctly different than other heavy metals as it significantly reduced at 700 °C, which may occur due to evaporation of Cd at around 700 °C [26]. The total concentrations of Zn and Ni were also reduced by considerable amounts at 900 °C, which may occur due to vaporization of Zn and evaporation of Ni containing compounds such as nickel carbonyl or nickel chloride or due to carryover of metal-containing particles to the gas stream. However, it needs to be investigated further to find out why other metals were not affected by this phenomena. Therefore, 900 °C is not suitable as some heavy metal including components may emit to atmosphere. These emissions are toxic, hence temperatures 500 °C and 700 °C are more suitable for

pyrolysis and co-pyrolysis as most heavy metal are retained in the biochar without emitting to the atmosphere. Also, biochar can have several non-agriculture applications such as adsorbent, catalyst and construction material where presence of metals may not be a limiting factor.

Biochar produced from co-pyrolysis of biosolids with alum sludge contained significantly lower concentrations of Cd, Cr, Cu, Pb, Se and Zn compared to biochar produced from pyrolysis of biosolids and concentrations of these heavy metals further decreased with increasing alum sludge mixing ratio. This decrease of heavy metals in co-pyrolysis biochar might be brought about by dilution effect due to the addition of alum sludge which has a considerably lower concentration of Cd, Cr, Cu, Pb, Se and Zn compared to biosolids. Concentrations of Cd and Se in biochar produced from co-pyrolysis of biosolids with alum sludge at 3:1 mixing ratio were within the limits required for unrestricted land applications from EPA Victoria. Even though Cu and Zn concentrations were still higher than the limits required for unrestricted land applications, their concentrations reduced significantly in co-pyrolysis biochar. For example, at 700 °C, Cu concentration reduction in biochar amounted to 51.55% in AS: BS 1:1% and 79.33% in AS: BS 3:1 compared to biosolids biochar. Similarly, Zn concentration reduction amounted to 57.16% in AS: BS 1:1% and 79.67% in AS: BS 3:1 compared to biosolids biochar. Therefore, it can be seen co-pyrolysis of biosolids with alum sludge reduced heavy metal concentration in biochar by a significant amount. Even though this reduction was insufficient to produce Grade C1 biochar, it is evident that co-pyrolysis of biosolids with alum sludge improved the quality of biochar by reducing heavy metal content.

3.1.3. DTPA extractable heavy metal concentrations in biochar

Biochar with lower total heavy metal concentrations are preferred by Regulators in soil application, but higher total heavy metal concentration do not necessarily mean more harm as most of the heavy metal present in biochar are stable and not bioavailable. Therefore, DTPA extractable heavy metal concentration is a more suitable indicator to represent bioavailable heavy metal concentration. Table 2 includes the DTPA extractable heavy metals (Cd, Cu, Ni, Pb and Zn) in biosolids, alum sludge and their resultant biochar. The DTPA extraction method is used for estimating the potential soil availability(bioavailable) of heavy metals. DTPA extractable concentrations of the considered heavy metals were significantly lower in the biochar compared to their raw material. This indicates that pyrolysis and co-pyrolysis reduce extractable heavy metal concentrations by significant amounts, and it is consistent with the observations from other studies in literature [4,27]. Yang et al. and

Table 2
DTPA extracted heavy metal concentration in feedstocks and resultant biochar from pyrolysis and co-pyrolysis experiments.

Metal Component	Metal content (mg/kg)													
	Temperature		500 °C				700 °C				900 °C			
	Biosolids	Alum sludge	BSBC	ASBC	AS:BS (1:1) BC	AS:BS (3:1) BC	BSBC	ASBC	AS:BS (1:1)BC	AS:BS (3:1) BC	BSBC	ASBC	AS:BS (1:1)BC	AS:BS (3:1) BC
Cd	0.60 ± 0.36	< 0.01	0.05 ± 0.03	< 0.01	< 0.01	0.015 ± 0.05	< 0.01	< 0.01	< 0.01	< 0.01	< 0.01	< 0.01	< 0.01	< 0.01
Cu	332.85 ± 80.13	0.81 ± 0.32	42.65 ± 9.77	0.36 ± 0.40	27.47 ± 4.32	1.02 ± 0.45	29.87 ± 9.51	0.71 ± 0.27	16.47 ± 6.12	3.71 ± 0.83	32.27 ± 5.42	0.25 ± 0.34	13.54 ± 6.73	3.69 ± 1.56
Ni	5.47 ± 0.97	0.70 ± 0.51	0.51 ± 0.65	0.09 ± 0.50	0.28 ± 0.41	0.11 ± 0.57	0.08 ± 0.21	0.06 ± 0.26	0.54 ± 0.08	0.008 ± 0.005	0.39 ± 0.58	0.05 ± 0.49	0.12 ± 0.33	0.09 ± 0.03
Pb	1.14 ± 0.72	0.25 ± 0.76	0.67 ± 0.09	0.018 ± 0.015	0.01 ± 0.09	0.34 ± 0.97	0.34 ± 0.97	0.01 ± 0.01	0.30 ± 0.66	0.22 ± 0.36	0.97 ± 0.75	0.01 ± 0.08	0.34 ± 0.87	0.02 ± 0.03
Zn	404.37 ± 36.76	2.13 ± 0.83	38.43 ± 3.67	0.21 ± 0.39	22.32 ± 5.53	8.5 ± 3.99	32.65 ± 8.43	0.16 ± 0.08	12.31 ± 1.87	9.55 ± 0.75	39.88 ± 5.63	0.21 ± 0.09	8.77 ± 9.87	8.26 ± 2.06

BSBC = Biosolids biochar, ASBC = Alum sludge biochar, AS: BS (1:1) BC= Biochar from co-pyrolysis of alum sludge and biosolids at 1:1 mixing ratio, AS: BS (3:1) BC= Biochar from co-pyrolysis of alum sludge and biosolids at 3:1 mixing ratio

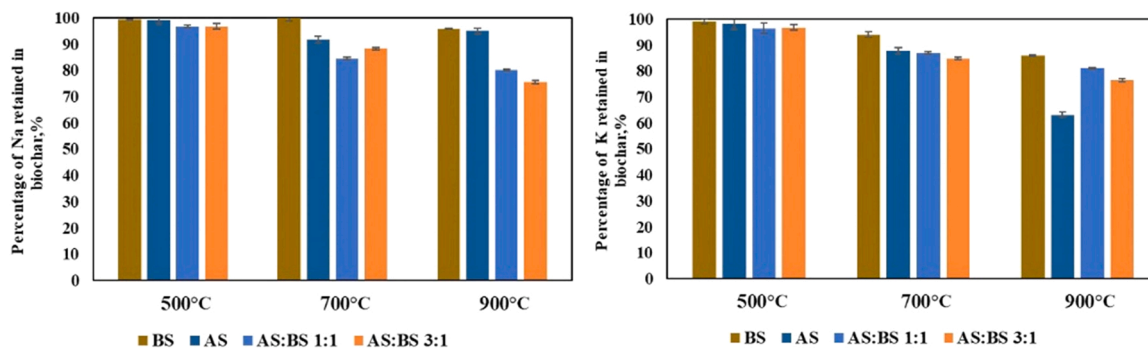


Fig. 3. Retention of Na and K in biochar produced from pyrolysis and co-pyrolysis at different pyrolysis temperatures (500 °C, 700 °C, and 900 °C).

Table 3

The ultimate and proximate analysis of feedstocks and resultant biochar from pyrolysis co-pyrolysis experiments on dry basis.

Temperatures		500 °C						700 °C				900 °C			
Samples		Biosolids	Alum Sludge	BSBC	ASBC	AS:BS (1:1) BC	AS:BS (3:1) BC	BSBC	ASBC	AS:BS (1:1) BC	AS:BS (3:1) BC	BSBC	ASBC	AS:BS (1:1) BC	AS:BS (3:1) BC
Ultimate analysis (wt%)	C	36.71 ± 1.39	12.18 ± 0.59	29.26 ± 1.00	11.29 ± 0.37	19.49 ± 0.04	15.51 ± 1.23	26.46 ± 0.67	10.44 ± 0.06	17.31 ± 1.94	12.51 ± 0.97	25.81 ± 0.09	8.54 ± 0.02	14.83 ± 1.00	6.31 ± 1.76
	H	4.24 ± 0.58	5.82 ± 0.17	1.33 ± 0.02	2.37 ± 1.08	1.05 ± 0.12	0.93 ± 0.05	1.03 ± 0.05	2.16 ± 0.70	1.01 ± 0.10	0.19 ± 0.40	0.86 ± 0.13	2.09 ± 0.33	0.80 ± 0.17	0.50 ± 0.23
	N	5.42 ± 0.46	1.26 ± 0.13	3.62 ± 0.13	1.16 ± 0.02	2.16 ± 0.05	1.22 ± 0.23	3.33 ± 0.16	0.99 ± 0.10	2.04 ± 0.23	1.13 ± 0.05	3.08 ± 0.50	0.87 ± 0.12	1.34 ± 0.15	0.63 ± 0.46
	S	0.92 ± 0.09	0.68 ± 0.18	0.24 ± 0.18	0.22 ± 0.05	0.37 ± 0.08	0.65 ± 0.10	0.52 ± 0.03	0.32 ± 0.07	0.3 ± 0.11	0.42 ± 0.06	0.42 ± 0.04	0.32 ± 0.02	0 ± 0.11	0.12 ± 0.08
O ^d		23.70 ± 0.89	23.06 ± 0.31	11.47 ± 1.00	12.52 ± 0.33	8.93 ± 0.47	11.31 ± 1.63	8.35 ± 0.67	9.55 ± 0.48	8.41 ± 1.22	9.12 ± 2.28	5.49 ± 1.56	5.10 ± 1.33	5.86 ± 0.56	11.78 ± 1.36
	H/C	1.39 ± 0.22	5.73 ± 0.10	0.55 ± 0.02	2.52 ± 1.00	0.65 ± 0.07	0.72 ± 0.01	0.83 ± 0.01	2.48 ± 0.78	0.70 ± 0.01	0.18 ± 0.32	0.86 ± 0.06	2.94 ± 0.46	0.73 ± 0.08	0.95 ± 0.12
HHV (MJ/kg)		14.68 ± 0.24	8.81 ± 0.42	9.93 ± 0.46	5.53 ± 1.60	5.56 ± 0.24	4.74 ± 0.58	9.17 ± 0.31	5.51 ± 0.90	5.43 ± 0.98	2.69 ± 1.15	9.07 ± 0.45	5.31 ± 0.57	5.53 ± 0.62	2.76 ± 1.08
	pH	6.80 ± 0.35	7.32 ± 0.40	9.13 ± 0.37	9.51 ± 0.30	9.16 ± 0.31	9.93 ± 0.30	9.56 ± 0.21	10.39 ± 0.37	9.22 ± 0.44	10.54 ± 0.27	10.11 ± 0.27	11.07 ± 0.25	9.49 ± 0.27	10.85 ± 0.52
Proximate analysis (wt%)	Volatile Matter	55.7 ± 1.00	27.12 ± 0.34	17.74 ± 0.10	12.92 ± 0.82	15.27 ± 0.21	13.39 ± 0.37	12.11 ± 3.00	10.79 ± 0.88	11.19 ± 1.07	10.28 ± 0.58	15.34 ± 1.28	6.72 ± 0.64	10.88 ± 0.17	8.3 ± 0.40
	Ash	28.43 ± 0.29	56.23 ± 0.29	54.08 ± 0.05	72.44 ± 1.11	68.00 ± 0.28	70.38 ± 0.35	60.3 ± 0.04	76.54 ± 1.20	70.93 ± 0.70	76.63 ± 0.73	64.34 ± 1.84	83.08 ± 0.89	77.17 ± 0.86	80.66 ± 0.44
	Fixed Carbon	15.81 ± 1.29	16.65 ± 0.05	28.18 ± 1.00	14.64 ± 1.93	16.73 ± 0.49	16.22 ± 0.09	27.59 ± 3.11	12.67 ± 2.08	17.88 ± 1.77	13.09 ± 0.15	10.32 ± 0.56	10.20 ± 0.25	11.95 ± 1.03	11.04 ± 0.04

BSBC = Biosolids biochar, ASBC = Alum sludge biochar, AS: BS (1:1) BC= Biochar from co-pyrolysis of alum sludge and biosolids at 1:1 mixing ratio, AS: BS (3:1) BC= Biochar from co-pyrolysis of alum sludge and biosolids at 3:1 mixing ratio

^d Calculated by difference

Jiang et al. have mentioned that one of the possible explanations for this reduction may be the development of functional groups on biochar surfaces that result in immobilization of heavy metals due to the formation of organic-metallic complexes [4,27].

Co-pyrolysis of biosolids with alum sludge also reduced the DTPA extractable heavy metal concentrations in biochar compared to biosolids biochar and increasing the mixing ratio of alum sludge further reduced the extractable heavy metal concentrations. This can be due to the reduction of the total concentration of heavy metals in co-pyrolysis biochar and further reduction of total heavy metal concentrations with increasing alum sludge mixing ratio. DTPA extractable heavy metals in biochar did not show a specific trend with pyrolysis and co-

pyrolysis temperature. However, it was observed from the previous section (Table 1) that total heavy metal concentration for most of the heavy metal components in biochar increased with pyrolysis/co-pyrolysis temperature up to 700 °C. Also, according to literature, higher pyrolysis/co-pyrolysis temperatures increased the immobilization of unstable metals, which might reduce DTPA extractable heavy metal concentrations [1,13,20].

3.1.4. Alkali metal retained in biochar

Percentages of Na and K retained in biochar produced from pyrolysis/co-pyrolysis of biosolids and alum sludge are shown in Fig. 3. This figure indicates that the majority of alkali metals were retained in

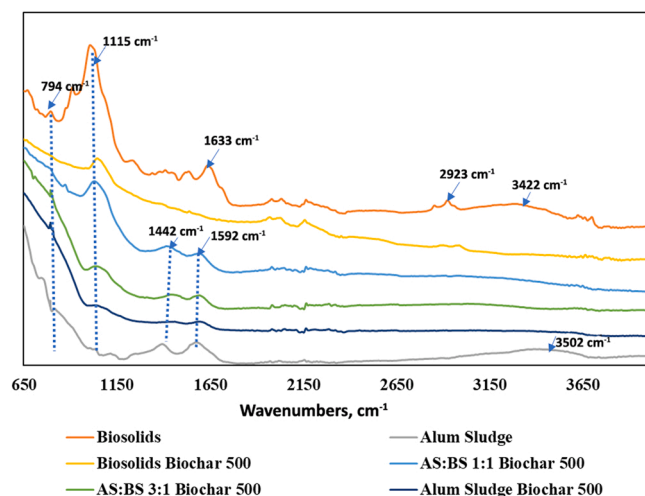


Fig. 4. FTIR spectra of biochar prepared at different mixing ratios of biosolids and alum sludge at 500 °C pyrolysis temperature.

biochar after pyrolysis and co-pyrolysis of biosolids and alum sludge. Retainment of alkali metals in biochar is important as release of alkali metals into gaseous products during pyrolysis/co-pyrolysis is detrimental which may cause several issues such as ash accumulation, slagging, and corrosion in the pyrolysis/co-pyrolysis reactor [28].

According to Fig. 3, percentage of alkali metal retained in biochar reduced with temperature, especially at 900 °C. This effect was significant in Na retained in biochar derived from co-pyrolysis at AS:BS 3:1 mixing ratio, where the percentage of Na retained reduced from 96.67% to 75.53% in 500–900 °C. During pyrolysis, only loosely bonded free ions are released, while at high temperatures, more strongly bonded alkali metals may decompose, which explains the decrease in the percentage of Na and K retained in biochar with rising temperatures [28]. It can also be observed that K release during pyrolysis of alum sludge at 900 °C was significant. K release during pyrolysis depends on pyrolysis temperature and feedstock composition [29,30]. When feedstock has high chlorine concentration high K release can be observed and when high amount of Si is present higher retention of K can be observed [29–31]. Therefore, the possible explanation for this phenomena is the sublimation of KCl at temperatures higher than 700 °C, due to higher concentration of Cl present in Alum Sludge [29,30]. Higher K retention in biosolids pyrolysis and biosolids and alum sludge co-pyrolysis with comparison to alum sludge pyrolysis may be contributed to high Si and S content present in biosolids.

Percentages of Na retained in biosolids biochar ranged from 99.30% to 95.8%, and alum sludge biochar ranged from 99.12% to 95.10% while AS: BS 1:1 biochar ranged from 96.76% to 80.19% and AS:BS 3:1 ranged from 96.67% to 75.53%. A similar trend can be observed in K retention in pyrolysis and co-pyrolysis biochar, but the decrease of K

Table 4

BET surface area of feedstocks and biochar produced from pyrolysis/co-pyrolysis of biosolids and alum sludge.

Biochar sample	Pyrolysis/ Co-pyrolysis temperature (°C)	BET surface area (m ² /g)
BSBC	500	29.34 ± 0.68
	700	89.32 ± 1.11
	900	33.85 ± 1.36
ASBC	500	18.21 ± 0.77
	700	35.18 ± 2.19
	900	15.51 ± 0.84
AS:BS (1:1)BC	500	22.05 ± 0.71
	700	40.90 ± 2.44
	900	17.54 ± 0.04
AS:BS (3:1)BC	500	18.71 ± 0.51
	700	24.52 ± 0.91
	900	14.00 ± 0.02
BS	–	3.06 ± 0.16
AS	–	7.95 ± 1.38

retention in co-pyrolysis biochar was less significant. Further investigation is required to explain this behavior in co-pyrolysis of biosolids with alum sludge.

3.1.5. General properties of biochar

Proximate and ultimate analysis, pH and higher heating value (HHV) of feedstock and resultant biochar products are summarized in Table 3. As the pyrolysis/co-pyrolysis temperature increased, volatile matter content decreased, and ash content increased in biochar products from all feedstock. This observation is consistent with the available literature data and can be attributed to more organic matter in biosolids being decomposed at higher temperatures leading to lower volatile matter content in the resultant biochar [9,20,23,24]. It can also be observed that biochar produced from co-pyrolysis had a significantly lower volatile matter and higher ash contents compared to biochar derived from biosolids pyrolysis, and the volatile matter was further decreased and ash content further increased with increasing alum sludge mixing ratio. This can be explained by the significantly lower organic matter and higher ash content in alum sludge compared to biosolids.

The pH value of biosolids were slightly acidic at 6.80, and pH values of biochar were higher after pyrolysis compared to the feedstocks, and the increasing temperature produced biochar with higher alkalinity. The possible reason for this phenomenon may be due to the increased decomposition of organic matters at higher temperatures which leads to higher concentration of alkali salts in the biochar. Biochar produced from co-pyrolysis of biosolids and alum sludge were also alkaline, and higher pH values were observed in biochar prepared at higher alum sludge mixing ratio. Higher pH value of co-pyrolysis biochar can be attributed to high ash content in alum sludge. Therefore, biochar produced from pyrolysis/co-pyrolysis of biosolids and alum sludge might lead to improved soil fertility via raising soil pH and the concomitant benefits on soil nutrient availability, particularly in acidic soils.

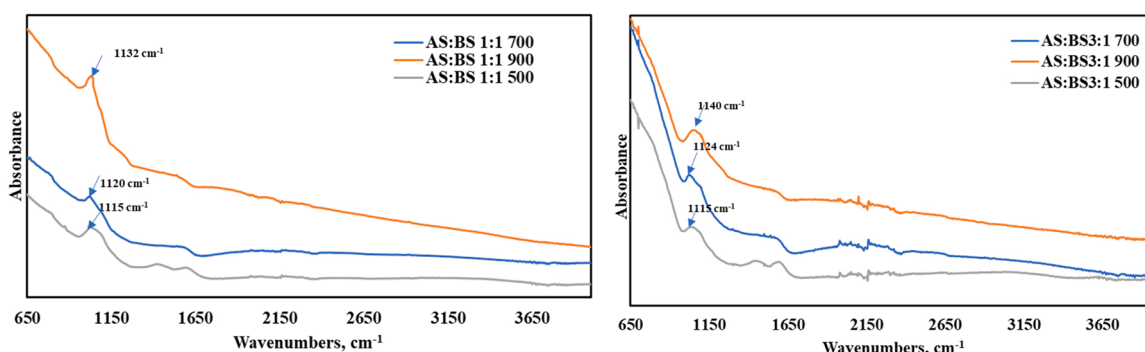


Fig. 5. FTIR spectra of co-pyrolysis biochar prepared at different temperatures (500 °C, 700 °C, and 900 °C).

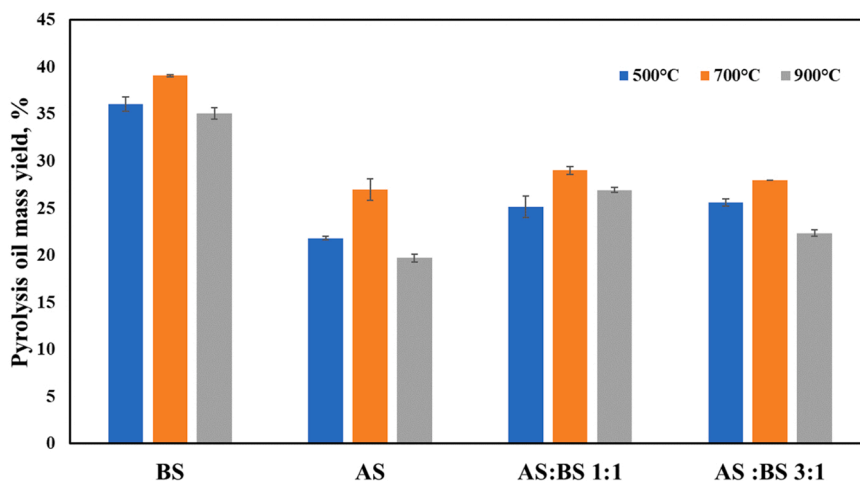


Fig. 6. Mass yield of liquid product from pyrolysis/co-pyrolysis of alum sludge and biosolids at different pyrolysis temperatures (500 °C, 700 °C, and 900 °C).

3.1.6. FTIR analysis of biochar

FTIR spectra of raw biosolids, alum sludge and biochar produced from pyrolysis and co-pyrolysis of biosolids and alum sludge at 500 °C are presented in Fig. 4. In raw biosolids FTIR spectra, a wide peak with a maximum at 3422 cm⁻¹ indicates OH and NH stretching vibrations, the peak in 2923 cm⁻¹ indicates CH₃ asymmetric stretch vibrations, and bands at 1633 cm⁻¹ and 1560 cm⁻¹ can be attributed to the presence of amides and -C=O groups [5,9,13,32,33]. In alum sludge FTIR spectra, peaks at 1115 cm⁻¹ and 794 cm⁻¹ indicate symmetric stretching vibration of Si—O—Si and bending vibration of O—Si—O [34,35]. Peaks at 1592 cm⁻¹ and 3502 cm⁻¹ alum sludge spectra may indicate the bending vibration of water that are chemically bonded to Al (OH)₃ or OH stretching vibration of Al(OH)₃ [34,35]. The absorption band at 1442 cm⁻¹ indicates the presence of carbonate [34,35]. Compared with biosolids and alum sludge, many peaks reduced or completely disappeared in biochar, and the peak intensities further reduced at higher temperatures. O-H peak disappeared in biochar and C-H vibration were reduced in biochar derived from pyrolysis and gradually disappeared with increasing pyrolysis temperature. This suggested that large amounts of hydroxyl groups and aliphatic compounds were decomposed in pyrolysis, and elevated pyrolysis temperatures promoted further degradation [5]. However, it can be observed that aromatic C-O stretching (1034 cm⁻¹) and aromatic C = O (794 cm⁻¹) were quite stable in pyrolysis [5]. It can also be seen that in biochar produced from co-pyrolysis and pyrolysis of alum sludge peaks corresponding to Si—O—Si stretching and carbonate were still stable and as can be seen

from Fig. 5 the peak corresponding to Si—O—Si stretching shifted slightly to higher wave numbers at higher temperatures, which indicates the changes in bonding structure of silicate network which could result into crystallization of silica [34,35].

3.1.7. Surface morphology of biochar

BET surface area of biosolids, alum sludge and biochar produced from pyrolysis and co-pyrolysis of biosolids and alum sludge are presented in Table 4. It is evident that pyrolysis and co-pyrolysis improved the surface area, as the BET surface area of all the biochar are significantly improved compared to biosolids and alum sludge. Biochar produced from pyrolysis of alum sludge and co-pyrolysis of biosolids and alum sludge have significantly lower surface area than biochar derived from biosolids pyrolysis. The surface area of co-pyrolysis biochar also decreased with increasing alum sludge mixing ratio in biochar. This can be attributed to the lower volatile matter present in alum sludge when compared to biosolids.

It can also be observed that BET surface area of biochar generally improved with increasing pyrolysis/co-pyrolysis temperature. This can be explained by the further degradation of organic materials present in biochar at higher pyrolysis and co-pyrolysis temperatures. However, there is a sharp decline in the BET surface from 700 °C to 900 °C. This can be explained by pores in biochar being blocked at high temperatures due to sintering and this observation is consistent with existing literature [1,5,9].

These results are further confirmed by the SEM images of the biochar

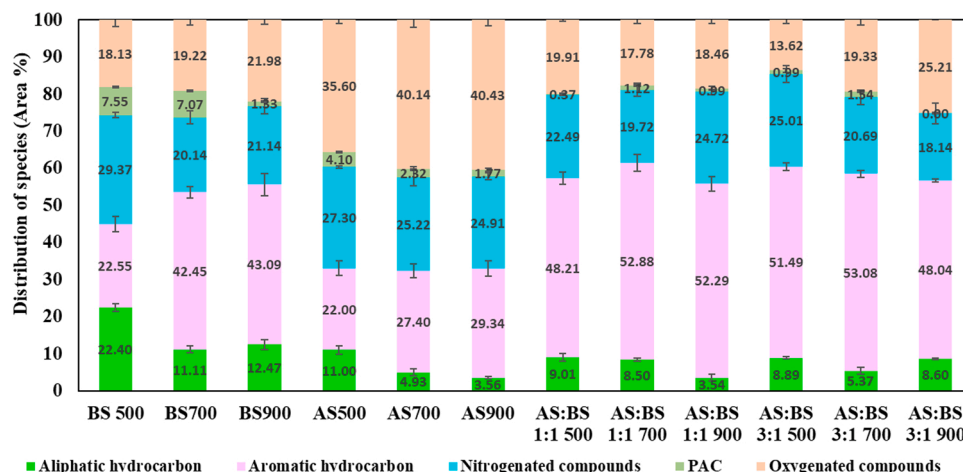


Fig. 7. Composition of pyrolysis/co-pyrolysis oil produced at different temperatures (500 °C, 700 °C, and 900 °C) and mixing ratios.

as shown in supplementary data (Fig. S2, S3 and S4). It is evident that when compared with alum sludge biochar, biosolids biochar have a better developed and well-defined crystalline structure. Alum sludge biochar is amorphous and granular, with irregular packed flake-like particles, and there are visible cracks in alum sludge biochar which suggests lower thermal stability. It is visible that biochar obtained from co-pyrolysis of biosolids with alum sludge basically contained a mix of biochar from biosolids pyrolysis and biochar from alum sludge pyrolysis which also explains the intermediate values of BET surface area in co-pyrolysis biochar.

3.2. Pyrolysis oil yield and characterization

Pyrolysis oil yield from pyrolysis and co-pyrolysis of biosolids at 500 °C, 700 °C and 900 °C are presented in Fig. 6. Pyrolysis oil mass yield from pyrolysis/co-pyrolysis of biosolids and alum sludge increased with rising pyrolysis temperatures up to 700 °C and then slightly decreased at 900 °C. This phenomenon is consistent with the literature data and can be explained by two factors [5,36]. De-volatilization of organic matter increased at elevated temperatures leading to a higher yield of volatile products thereby increasing oil yield. Conversely, at higher temperatures, significant gas phase secondary reactions occur, which promotes gas production leading to a reduction in the oil yield.

Alum sludge pyrolysis produced less pyrolysis oil yield than pyrolysis of biosolids. This can be explained by less volatile matter present in alum sludge in comparison to biosolids. As seen from Fig. 6, the oil yield results for co-pyrolysis at AS:BS (1:1) were significantly lower than oil yield from biosolids pyrolysis and it further decreased with increasing alum sludge mixing ratio. This may occur as feedstock mixtures used in co-pyrolysis contains less volatile content than biosolids due to alum sludge addition. Additionally, the mineral content present in alum sludge may contribute to reduction of oil product by promoting tar cracking reactions [37–39]. Lower oil product from co-pyrolysis is beneficial in reducing undesired tar production that can cause plugging, fouling, and corrosion in pipelines in pyrolysis/co-pyrolysis reactors [40].

The GC/MS analysis of pyrolysis oils revealed that they comprise of complex mixture of organic compounds as shown in supplementary data (Table S1). The composition of the compounds in pyrolysis oil was calculated based on the area of peaks from GC/MS analysis, where the species were categorized into five groups, namely aliphatic hydrocarbon, aromatic hydrocarbon, nitrogenated compounds, oxygenated compounds and polyaromatic compounds (PAC). This categorization was based on several previous studies [5,41,42]. Alkanes, alkenes and their derivatives are categorized as the aliphatic hydrocarbons while benzene and its derivatives, phenols, and its derivatives as well as furans form the aromatics group, and compounds such as naphthalene and indene constitute the PACs group [5,41,42]. Nitrogenated compounds

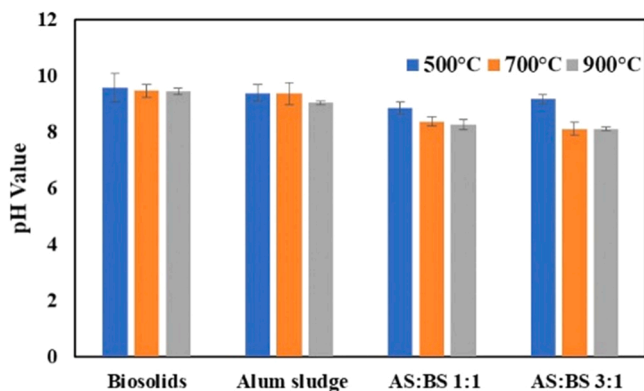


Fig. 8. pH values of pyrolysis/co-pyrolysis oil produced at different temperatures (500 °C, 700 °C, and 900 °C) and mixing ratios.

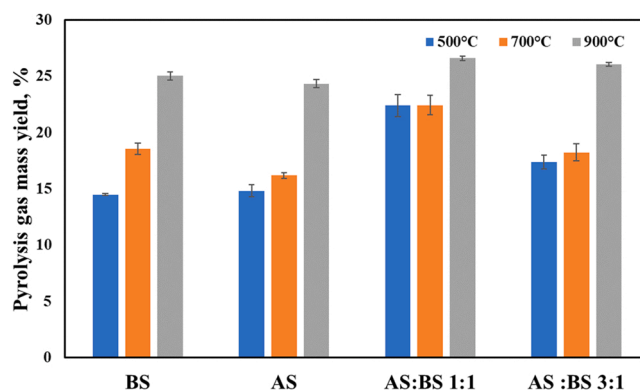


Fig. 9. Mass yield of pyrolysis gas from pyrolysis/co-pyrolysis of alum sludge and biosolids at different temperatures (500 °C, 700 °C, and 900 °C) and mixing ratios.

contain amines and amides such as pyridine, pyrazole and imidazole, while oxygenated compounds include aldehydes, ketones, esters and carboxylic acids [5,41,42].

Fig. 7 illustrates the distribution of pyrolysis oil compounds from pyrolysis/co-pyrolysis of biosolids and alum sludge. This analysis indicates that the composition of pyrolysis oil varies with feedstock mixture and pyrolysis /co-pyrolysis temperature. However, according to Fig. 7, all the pyrolysis oil studied mainly contains aromatic hydrocarbons, oxygenated compounds and nitrogenated compounds. PAC was found in significantly lower quantities, but the presence of PAC is highly undesirable. High amount of nitrogenated components in pyrolysis oil also significantly limits its application as a liquid fuel. But according to several studies, nitrogenated components in pyrolysis oil can be reduced by using catalysts [5,12,18,43]. Alternatively, these pyrolysis oils can be used as a source of chemical compounds to produce nitrogen-containing fertilizer [43].

Moreover, with increasing pyrolysis temperature, composition of aromatic hydrocarbons and oxygenated compounds increased while aliphatic hydrocarbon and nitrogenated compounds decreased. Thermal cracking of nitrogenated compounds at increased temperatures are presumable, which may lead to the decrease of nitrogenated compounds in pyrolysis oil. Decrease in aliphatic hydrocarbons and increase in aromatic hydrocarbons may occur due to the increase in dehydrogenation reactions at higher temperatures leading to decompose of large aliphatic hydrocarbons to produce aromatic hydrocarbons and hydrogen at high temperatures [43]. Formation of PAC also decreased with increasing pyrolysis/co-pyrolysis temperature, and these findings are consistent with literature [5].

Similarly, compositions of aromatic hydrocarbons and oxygenated compounds increased while aliphatic hydrocarbon and nitrogenated compounds decreased when co-pyrolysis of biosolids was performed with alum sludge. These effects increased with the increasing mixing ratio of alum sludge. Mineral compounds present in alum sludge acting as catalysts in cracking reactions and denitrogenation and dehydrogenation reactions may explain these effects on pyrolysis oil composition. Thus, co-pyrolysis slightly increased the oil product quality due to the decrease in polyaromatic compounds and nitrogenated compounds. However, a significant amount of nitrogenated compounds are still present in oil produced from co-pyrolysis, and upgrading is necessary before using it as a liquid fuel.

pH values of pyrolysis oil produced from pyrolysis/co-pyrolysis of biosolids and alum sludge are shown in Fig. 8. All the oil samples produced from pyrolysis and co-pyrolysis of biosolids and alum sludge had basic values in the range of 8.8–9.7. pH values of pyrolysis oils represent the corrosiveness of oil and fuel acidity of pyrolysis oil produced from lignocellulosic biomass is a main concern in using it as a fuel because of its corrosive character [43]. The possible explanation for the basic pH

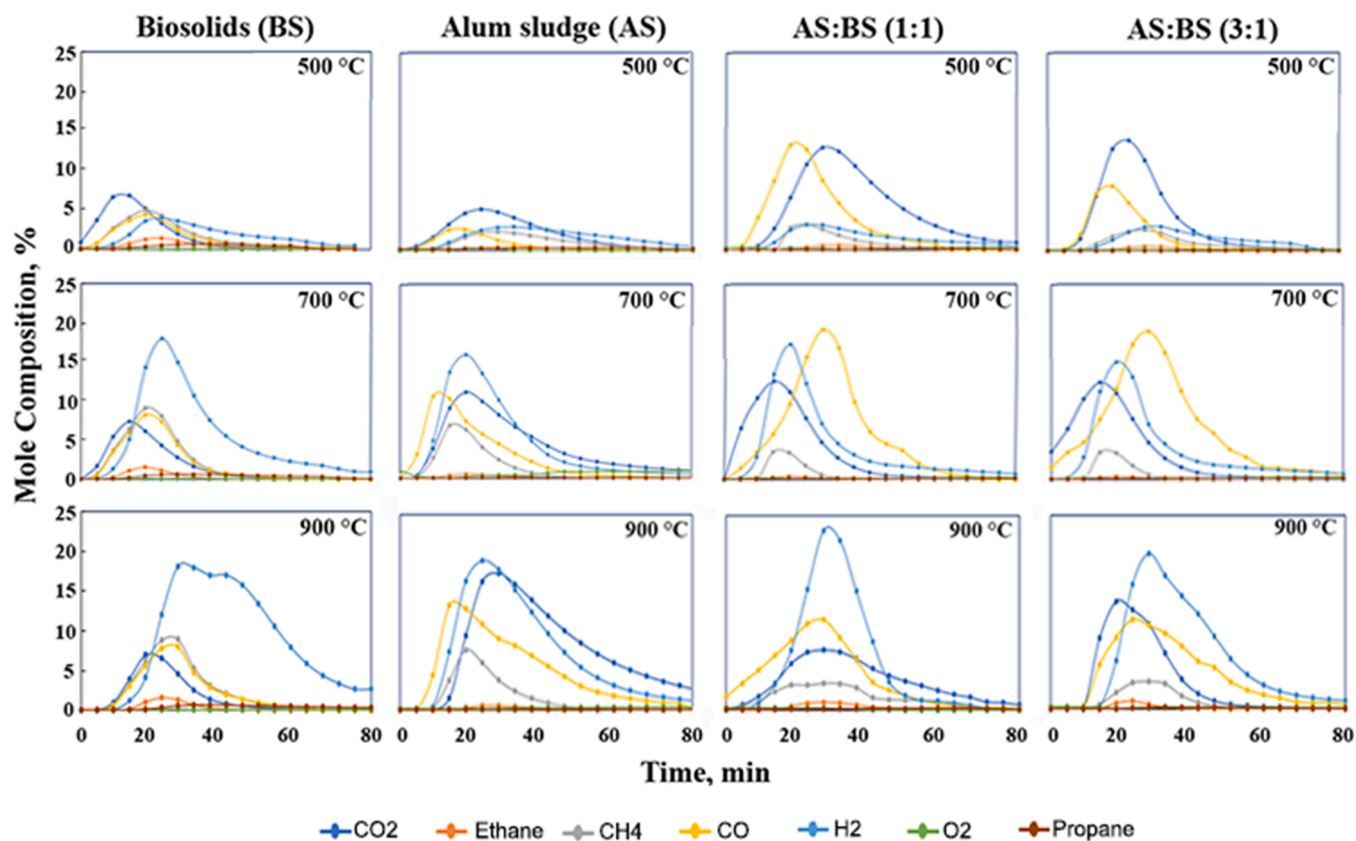


Fig. 10. Composition of gas products from pyrolysis and co-pyrolysis of alum sludge and biosolids.

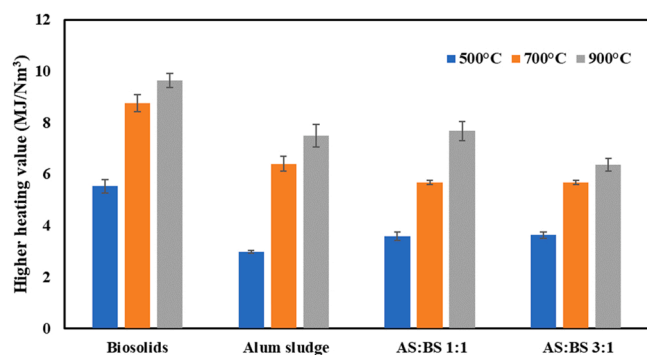


Fig. 11. Higher heating value of pyrolysis gas produced from pyrolysis/co-pyrolysis of biosolids and alum sludge at different temperatures (500 °C, 700 °C, and 900 °C).

values in oil derived from pyrolysis and co-pyrolysis of biosolids and alum sludge may be the presence of high amount of N containing compounds [43].

3.3. Pyrolysis gas yield and characterization

Gas yield from pyrolysis/co-pyrolysis of biosolids and alum sludge at 500 °C, 700 °C and 900 °C are presented in Fig. 9. Gas mass yield from pyrolysis/co-pyrolysis of biosolids and alum sludge increased with increasing temperature. This phenomenon is consistent with the literature data and can be explained by two factors [5,38,44,45]. De-volatilization of organic matter increased with temperature leading to a higher yield of volatile products, thereby increasing gas yield. Furthermore, at higher temperatures, significant gas phase secondary reactions occur, which promotes gas production [5,38,44,45].

Alum sludge pyrolysis produced less pyrolysis gas yield than pyrolysis of biosolids. This can be explained by less volatile matter present in alum sludge in comparison to biosolids. It was expected co-pyrolysis would result gas yields intermediate to the gas yield from individual pyrolysis of biosolids and alum sludge as co-pyrolysis feed stock mixtures used in co-pyrolysis contains less volatile content than biosolids and more volatile content than alum sludge. As seen from Fig. 9, the pyrolysis gas yield results for co-pyrolysis were higher than the yield obtained from individual pyrolysis of alum sludge and biosolids. Unexpected increase in gas yield in co-pyrolysis may occur due to the catalytic effect of minerals present in alum sludge which promoted further degradation of large hydro carbons in char and oil to produce smaller gaseous components and low volatile content present in the feedstock mixture may have reduced the increase in the gas yield at AS: BS (3:1) mixing ratio.

Fig. 10 presents the concentration of CO, CO₂, H₂, CH₄, C₂H₆ and C₃H₈ in the outlet stream of the pyrolysis reactor with time. The remainder in the outlet stream consists of nitrogen that is used as the fluidization gas. In the first 20 min, the reactor was heated to pyrolysis temperature and the temperature was maintained for 60 min. The concentration of pyrolysis gases increased in the 0–30 min period and then gradually decreased. At 80 min, pyrolysis gas concentration was negligible in all cases implying that 60 min residence time was sufficient for the completion of pyrolysis/co-pyrolysis reactions.

H₂, CO, CO₂ and CH₄ were the most abundant components in all pyrolysis conditions [46]. The composition of ethane and propane in gas outlet was significantly low and oxygen was only present in trace amounts. In biosolids pyrolysis, concentrations of H₂, CO, CO₂, CH₄, C₂H₆ and C₃H₈ generally increased with increasing temperature. This can be explained by the increase in pyrolysis gas production with increasing pyrolysis temperatures. This trend can be explained by high temperatures promoting dehydrogenation reactions which increases H₂ emission or secondary cracking of tar [36, 46–48]. Similar trends were

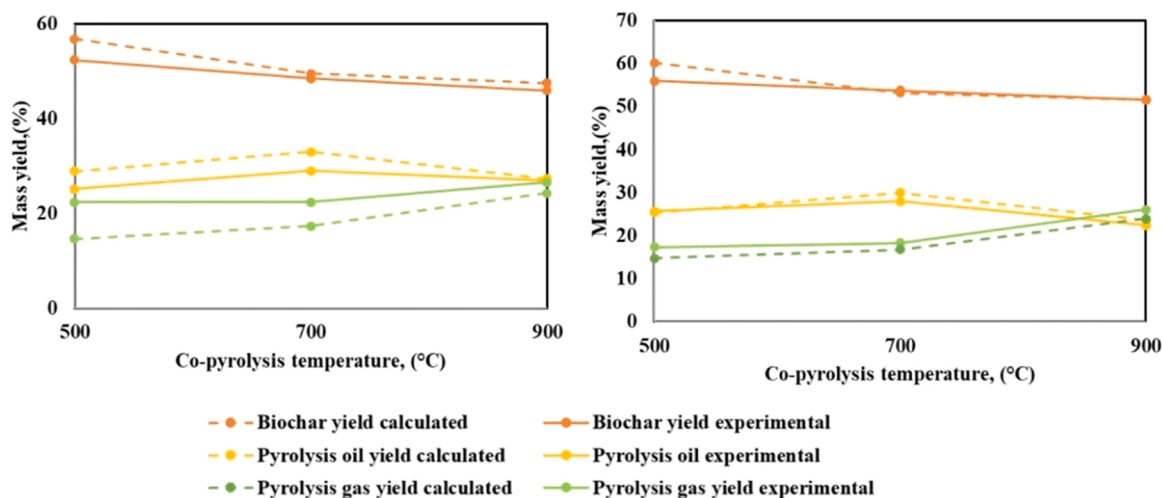


Fig. 12. Comparison of the experimental and calculated product yields of co-pyrolysis (a) AS: BS 1:1 (b) AS: BS 3:1 mixing ratios.

observed in alum sludge gas composition with increasing pyrolysis temperature. Concentrations of CO, H₂ and CO₂ increased from 8.93%, 2.93% and 5.12% at 500 °C to 13.94%, 19.68% and 18.39% at 900 °C, respectively.

Concentration of gas components in co-pyrolysis experiments displayed obvious synergistic effects. Gas production from co-pyrolysis was higher than gas production from pyrolysis in both biosolids and alum sludge. CO was the dominant component at 500 °C and 700 °C in both AS: BS (1:1) and AS: BS (3:1) mixing ratios but CO concentration slightly reduced at 900 °C. High CO concentration can be attributed to mineral components present in biosolids and alum sludge acting as catalysts to promote CO production in tar cracking reactions. H₂ concentration in co-pyrolysis gas was significantly higher than in H₂ content in biosolids, and alum sludge pyrolysis gas and H₂ content increased with increasing alum sludge mixing ratio.

Higher heating values (HHV) of the gas product from pyrolysis and co-pyrolysis of biosolids and alum sludge are presented in Fig. 11. It is clear that the heating value of the pyrolysis gases were influenced by the evolution of the hydrocarbons present in the gases. HHV of gas products in pyrolysis and co-pyrolysis in all feedstock increased with pyrolysis temperature. An increase in H₂ and CO with increasing temperature may have largely attributed to this trend. Pyrolysis gas produced from biosolids pyrolysis have a higher HHV than gas product from alum sludge pyrolysis. Gas product from co-pyrolysis of alum sludge and biosolids had lower HHV than biosolids pyrolysis, and the decrease in heating value with increasing alum sludge proportion was not significant in 500 °C and 700 °C.

3.4. Synergetic effect of co-pyrolysis of biosolids and alum sludge on co-pyrolysis behavior and product yields

Fig. 12 presents experimental and calculated product yields in co-pyrolysis of biosolids and alum sludge. In co-pyrolysis, experimental yield values of biochar and oil products were lower than the calculated value, while gas yield was higher than the calculated value. These synergistic effects may be due to the catalytic effect of AAEM (alkali and alkaline earth metals) and minerals in alum sludge which promotes promote char gasification, which reduces the biochar yield and increases gas yield [5,38,44,45]. The intensified secondary reaction may cause a reduction in oil yield while increasing gas yield [39]. It can also be seen that the presence of synergistic effects was more prominent in AS: BS (1:1) co-pyrolysis when compared to AS: BS (3:1). The possible explanation is that due to the low volatile matter present in the feedstock in co-pyrolysis at AS: BS 3:1 mixing ratio catalytic effect of AAEM earth metals and minerals are less obvious.

Interactions between feedstocks in co-pyrolysis were studied using a thermo gravimetric analyser and the results are shown Fig. S6. It was seen that biosolids pyrolysis occurs in three stages. First stage is dehydration which occurs between 50 °C and 180 °C. Devolatilization of carbohydrates and lipids occurs between 180 °C and 360 °C. Thermal degradation of protein, lignin and polymers occurs between 360 °C and 900 °C [5].

In alum sludge it can be seen that most mass decay occurs from 120 °C to 580 °C, which can be attributed to volatilization of the organic mass fraction in alum sludge and dehydration of Al(OH)₃. However, due to low organic content in alum sludge most of the mass decay is likely attributed to dehydration of Al(OH)₃ [5,21,22,34,35]. TGA curves for co-pyrolysis demonstrates an intermediate behavior to AS and BS. It can be seen that thermal degradation of AS starts at lower temperature than biosolids which indicated lower thermal stability. Also, gas analysis shows synergistic effects in co-pyrolysis. It was observed that co-pyrolysis of alum sludge and biosolids produces more CO, CO₂ and H₂ gases than individual pyrolysis of AS and BS. This can be explained by catalytic effect of alum sludge promoting char gasification and tar cracking reactions. This is also consistent with lower oil and biochar yield and higher gas yield in co-pyrolysis when compared to individual pyrolysis.

4. Conclusions

- In this study, the feasibility of using alum sludge as a feedstock to perform co-pyrolysis with biosolids to produce high quality biochar was studied. Compared to biochar derived from biosolids pyrolysis, the addition of alum sludge remarkably reduced the heavy metal concentrations present in biochar, especially Cu and Zn.
- Co-pyrolysis of biosolids with alum sludge produced a higher yield of biochar and gas compared to pyrolysis of biosolids.
- It was observed that heavy metal concentration in biochar reduced significantly with increasing alum sludge mixing ratio and biochar surface area, co-pyrolysis oil quality and gas yield and heating value generally increased with increasing temperature. However, at 900 °C, co-pyrolysis temperature it was observed that some heavy metals vaporized from biochar product which may pose environmental risks. Therefore, co-pyrolysis temperature of 700 °C and mixing ratio of 3:1 (alum sludge: biosolids) were identified as the most suitable conditions.
- Synergistic effects of co-pyrolysis of alum sludge with biosolids were observed in the product yields, which may attribute to catalytic effect of alumina and other minerals present in alum sludge.

CRedit authorship contribution statement

Conception and design of study: N. Rathnayake, K. Shah, S. Patel, acquisition of data: N. Rathnayake, S. Patel. analysis and/or interpretation of data: N. Rathnayake, P. Halder, S.Aktar, J. Pazferreiro, A. Surapaneni, A. Sharma. Drafting the manuscript: N. Rathnayake, revising the manuscript critically for important intellectual content: K. Shah, S. Patel, P. Halder, S.Aktar, J. Pazferreiro, A. Surapaneni, A. Sharma. Approval of the version of the manuscript to be published : N. Rathnayake, S. Patel, P. Halder, S. Aktar, J. Pazferreiro, A. Surapaneni, K. Shah, A. Sharma.

Declaration of Competing Interest

The authors declare that they have no known competing financial interests or personal relationships that could have appeared to influence the work reported in this paper.

Acknowledgments

The authors wish to acknowledge RMIT University, Australia, South East Water, Melbourne Water and Intelligent Water Networks (IWN) for the postgraduate scholarships and the financial assistance provided.

Appendix A. Supporting information

Supplementary data associated with this article can be found in the online version at [doi:10.1016/j.jaap.2022.105488](https://doi.org/10.1016/j.jaap.2022.105488).

References

- Z. Wang, X. Shu, H. Zhu, L. Xie, S. Cheng, Y. Zhang, Characteristics of biochars prepared by co-pyrolysis of sewage sludge and cotton stalk intended for use as soil amendments, *Environ. Technol.* 41 (11) (2020) 1347–1357, <https://doi.org/10.1080/09593330.2018.1534891>.
- p s d p. Ltd, "BIOSOLIDS SNAPSHOT," Department of Agriculture, Water and the Environment, Canberra ACT 2601, 2012. [Online]. Available: (<https://www.environment.gov.au/protection/waste/publications/biosolids-snapshot>).
- X.D. Song, X.Y. Xue, D.Z. Chen, P.J. He, X.H. Dai, Application of biochar from sewage sludge to plant cultivation: influence of pyrolysis temperature and biochar-to-soil ratio on yield and heavy metal accumulation, *Chemosphere* 109 (2014) 213–220, <https://doi.org/10.1016/j.chemosphere.2014.01.070>.
- Y. Yang, et al., Physicochemical properties of biochars produced from biosolids in Victoria, Australia, *Int J. Environ. Res Public Health* 15 (7) (2018), <https://doi.org/10.3390/ijerph15071459>.
- S. Patel, et al., Slow pyrolysis of biosolids in a bubbling fluidised bed reactor using biochar, activated char and lime, *J. Anal. Appl. Pyrolysis* 144 (2019), <https://doi.org/10.1016/j.jaap.2019.104697>.
- S. Patel, et al., A critical literature review on biosolids to biochar: an alternative biosolids management option, *Rev. Environ. Sci. Bio/Technol.* 19 (4) (2020) 807–841, <https://doi.org/10.1007/s11157-020-09553-x>.
- R.L.P. Karthik Rajendran, David M. Wall, Jerry D. Murphy, *Influent Aspects in Waste Management Practices. Sustainable Resource Recovery and Zero Waste Approaches*, 2019, pp. 65–78. Ch. 5.
- S. Kundu, et al., Removal of PFASs from biosolids using a semi-pilot scale pyrolysis reactor and the application of biosolids derived biochar for the removal of PFASs from contaminated water, *Environ. Sci. Water Res. Technol.* 7 (3) (2021) 638–649, <https://doi.org/10.1039/d0ew00763c>.
- Z. Wang, et al., Co-pyrolysis of sewage sludge and cotton stalks, *Waste Manag.* 89 (2019) 430–438, <https://doi.org/10.1016/j.wasman.2019.04.033>.
- N. Gao, K. Kamran, C. Quan, P.T. Williams, Thermochemical conversion of sewage sludge: a critical review, *Prog. Energy Combust. Sci.* 79 (2020), <https://doi.org/10.1016/j.pecs.2020.100843>.
- U.S. E.P. Agency, "Land Application of Biosolids." (<https://www.epa.gov/biosolids/land-application-biosolids>) (accessed 6/06/2021).
- F. Abnisa, W.M.A.Wan Daud, A review on co-pyrolysis of biomass: an optional technique to obtain a high-grade pyrolysis oil, *Energy Convers. Manag.* 87 (2014) 71–85, <https://doi.org/10.1016/j.enconman.2014.07.007>.
- H.-j Huang, T. Yang, F.-y Lai, G.-q Wu, Co-pyrolysis of sewage sludge and sawdust/rice straw for the production of biochar, *J. Anal. Appl. Pyrolysis* 125 (2017) 61–68, <https://doi.org/10.1016/j.jaap.2017.04.018>.
- X. Wang, B. Zhao, X. Yang, Co-pyrolysis of microalgae and sewage sludge: biocrude assessment and char yield prediction, *Energy Convers. Manag.* 117 (2016) 326–334, <https://doi.org/10.1016/j.enconman.2016.03.013>.
- B. Han, et al., Co-pyrolysis behaviors and kinetics of plastics–biomass blends through thermogravimetric analysis, *J. Therm. Anal. Calorim.* 115 (1) (2013) 227–235, <https://doi.org/10.1007/s10973-013-3228-7>.
- Z. Jin, L. Yin, D. Chen, Y. Jia, J. Yuan, Y. Hu, Co-pyrolysis characteristics of typical components of waste plastics in a falling film pyrolysis reactor, *Chin. J. Chem. Eng.* 26 (10) (2018) 2176–2184, <https://doi.org/10.1016/j.cjche.2018.07.005>.
- J.D. Martínez, et al., Co-pyrolysis of biomass with waste tyres: upgrading of liquid bio-fuel, *Fuel Process. Technol.* vol. 119 (2014) 263–271, <https://doi.org/10.1016/j.fuproc.2013.11.015>.
- S. Wang, et al., Co-pyrolysis and catalytic co-pyrolysis of Enteromorpha clathrata and rice husk, *J. Therm. Anal. Calorim.* 135 (4) (2018) 2613–2623, <https://doi.org/10.1007/s10973-018-7334-4>.
- X. Zhang, H. Lei, S. Chen, J. Wu, Catalytic co-pyrolysis of lignocellulosic biomass with polymers: a critical review, *Green Chem.* 18 (15) (2016) 4145–4169, <https://doi.org/10.1039/c6gc00911e>.
- J. Jin, et al., Cumulative effects of bamboo sawdust addition on pyrolysis of sewage sludge: biochar properties and environmental risk from metals, *Bioresour. Technol.* 228 (2017) 218–226, <https://doi.org/10.1016/j.biortech.2016.12.103>.
- D. Choi, J.I. Oh, J. Lee, Y.K. Park, S.S. Lam, E.E. Kwon, Valorization of alum sludge via a pyrolysis platform using CO₂ as reactive gas medium, *Environ. Int.* 132 (2019), 105037, <https://doi.org/10.1016/j.envint.2019.105037>.
- K.B. Dassanayake, G.Y. Jayasinghe, A. Surapaneni, C. Hetherington, A review on alum sludge reuse with special reference to agricultural applications and future challenges, *Waste Manag.* 38 (2015) 321–335, <https://doi.org/10.1016/j.wasman.2014.11.025>.
- T.Y. Hua-jun Huang, Fa-ying Laia, Guo-qiang Wu, Co-pyrolysis of sewage sludge and sawdust/rice straw for the production of biochar, *J. Anal. Appl. Pyrolysis* (2017), <https://doi.org/10.1016/j.jaap.2017.04.018>.
- X.S. Zhipu Wang, Henan Zhu, Like Xie, Shenhang Cheng, Yuxiu Zhang, Characteristics of biochars prepared by co pyrolysis of sewage sludge and cotton stalk intended for use as soil amendments, *Environ. Technol.* (2018), <https://doi.org/10.1080/09593330.2018.1534891>.
- R. Irwin, A. Surapaneni, D. Smith, J. Schmidt, H. Rigby, S.R. Smith, Verification of an alternative sludge treatment process for pathogen reduction at two wastewater treatment plants in Victoria, Australia, *J. Water Health* 15 (4) (2017) 626–637, <https://doi.org/10.2166/wh.2017.316>.
- R.C. Kistler, F. Widmer, P.H. Brunner, Behavior of chromium, nickel, copper, zinc, cadmium, mercury, and lead during the pyrolysis of sewage sludge, *Environ. Sci. Technol.* 21 (1987) 704–708, <https://doi.org/10.1021/es00161a012>.
- J. Jiang, R.K. Xu, Application of crop straw derived biochars to Cu(II) contaminated Ultisol: evaluating role of alkali and organic functional groups in Cu (II) immobilization, *Bioresour. Technol.* 133 (2013) 537–545, <https://doi.org/10.1016/j.biortech.2013.01.161>.
- J.L. Wenhan Cao, Leo Lue, Xiaolei Zhang, Release of alkali metals during biomass thermal conversion, *Arch. Ind. Biotechnol.* vol. 1 (1) (2016).
- J.M. Johansen, J.G. Jakobsen, F.J. Frandsen, P. Glarborg, Release of K, Cl, and S during pyrolysis and combustion of high-chlorine biomass, *Energy Fuels* 25 (11) (2011) 4961–4971, <https://doi.org/10.1021/ef201098n>.
- Z. Zhang, J. Liu, F. Shen, Z. Wang, Temporal release behavior of potassium during pyrolysis and gasification of sawdust particles, *Renew. Energy* 156 (2020) 98–106, <https://doi.org/10.1016/j.renene.2020.04.076>.
- K.V. Shah, M.K. Cieplik, C.I. Bertrand, W.L. van de Kamp, H.B. Vuthaluru, Correlating the effects of ash elements and their association in the fuel matrix with the ash release during pulverized fuel combustion, *Fuel Process. Technol.* 91 (5) (2010) 531–545, <https://doi.org/10.1016/j.fuproc.2009.12.016>.
- Y.Q. Yang, M.H. Cui, Y.G. Ren, J.C. Guo, Z.Y. Zheng, H. Liu, Towards understanding the mechanism of heavy metals immobilization in biochar derived from co-pyrolysis of sawdust and sewage sludge, *Bull. Environ. Contam. Toxicol.* vol. 104 (4) (2020) 489–496, <https://doi.org/10.1007/s00128-020-02801-4>.
- J. Zhang, F. Lu, H. Zhang, L. Shao, D. Chen, P. He, Multiscale visualization of the structural and characteristic changes of sewage sludge biochar oriented towards potential agronomic and environmental implication, *Sci. Rep.* 5 (2015) 9406, <https://doi.org/10.1038/srep09406>.
- M.Y. Soleha, et al., Characterization of raw and thermally treated alum sludge, *Key Eng. Mater.* 701 (2016) 138–142, <https://doi.org/10.4028/www.scientific.net/KEM.701.138>.
- M.A. Tantawy, Characterization and pozzolanic properties of calcined alum sludge, *Mater. Res. Bull.* 61 (2015) 415–421, <https://doi.org/10.1016/j.materresbull.2014.10.042>.
- M. Inguanzo, A. Domínguez, J.A. Menéndez, C.G. Blanco, J.J. Pis, On the pyrolysis of sewage sludge: the influence of pyrolysis conditions on solid, liquid and gas fractions, *J. Anal. Appl. Pyrolysis* 63 (1) (2002) 209–222, [https://doi.org/10.1016/s0165-2370\(01\)00155-3](https://doi.org/10.1016/s0165-2370(01)00155-3).
- K. Lan, Z. Qin, Z. Li, R. Hu, X. Xu, W. He, J. Li, Syngas production by catalytic pyrolysis of rice straw over modified Ni-based catalyst, *BioRes* (2020) 2293–2309.
- J. Zhu, Y. Yang, L. Yang, Y. Zhu, High quality syngas produced from the co-pyrolysis of wet sewage sludge with sawdust, *Int. J. Hydrog. Energy* 43 (11) (2018) 5463–5472, <https://doi.org/10.1016/j.ijhydene.2018.01.171>.
- X. Wang, et al., Synergetic effect of sewage sludge and biomass co-pyrolysis: a combined study in thermogravimetric analyzer and a fixed bed reactor, *Energy Convers. Manag.* 118 (2016) 399–405, <https://doi.org/10.1016/j.enconman.2016.04.014>.
- Y. Fan, et al., Minimizing tar formation whilst enhancing syngas production by integrating biomass torrefaction pretreatment with chemical looping gasification, *Appl. Energy* 260 (2020), <https://doi.org/10.1016/j.apenergy.2019.114315>.
- M.A.I. Fontes, L. Lazaro, G. Gea, M.B. Murillo, Gas chromatography study of sewage sludge pyrolysis liquids obtained at different operational conditions in a fluidized bed, *Ind. Eng. Chem. Res.* 48 (2009) 5907–5915, <https://doi.org/10.1021/ie900421a>.

- [42] C. Jindarom, V. Meeyoo, T. Rirksomboon, P. Rangsunvigit, Thermochemical decomposition of sewage sludge in CO₂ and N₂ atmosphere, *Chemosphere* 67 (8) (2007) 1477–1484, <https://doi.org/10.1016/j.chemosphere.2006.12.066>.
- [43] I. Fonts, G. Gea, M. Azuara, J. Abrego, J. Arauzo, Sewage sludge pyrolysis for liquid production: a review, *Renew. Sustain. Energy Rev.* 16 (5) (2012) 2781–2805, <https://doi.org/10.1016/j.rser.2012.02.070>.
- [44] X. Yang, C. Yuan, J. Xu, W. Zhang, Potential method for gas production: high temperature co-pyrolysis of lignite and sewage sludge with vacuum reactor and long contact time, *Bioresour. Technol.* 179 (2015) 602–605, <https://doi.org/10.1016/j.biortech.2014.11.104>.
- [45] W. Zhang, C. Yuan, J. Xu, X. Yang, Beneficial synergetic effect on gas production during co-pyrolysis of sewage sludge and biomass in a vacuum reactor, *Bioresour. Technol.* 183 (2015) 255–258, <https://doi.org/10.1016/j.biortech.2015.01.113>.
- [46] B. Zhang, S. Xiong, B. Xiao, D. Yu, X. Jia, Mechanism of wet sewage sludge pyrolysis in a tubular furnace, *Int. J. Hydrog. Energy* 36 (1) (2011) 355–363, <https://doi.org/10.1016/j.ijhydene.2010.05.100>.
- [47] A.J. Isabel Fonts, Gloria Gea, María B. Murillo, Jose L. Sanchez, Sewage sludge pyrolysis in fluidized bed, 1: influence of operational conditions on the product distribution, *Ind. Eng. Chem. Res.* 47 (2008) 5376–5385.
- [48] M.L.J.A. Menéndez, J.J. Pis, Microwave-induced pyrolysis of sewage sludge, *Water Res.* 36 (2002) 3261–3264.